European Journal of Pharmaceutics and Biopharmaceutics 74 (2010) 148–156

Contents lists available at ScienceDirect

European Journal of Pharmaceutics and Biopharmaceutics

journal homepage: www.elsevier.com/locate/ejpb

Research paper

A quantitative evaluation of the molecular binding affinity between a monoclonal antibody conjugated to a nanoparticle and an antigen by surface plasmon resonance

Nir Debotton [a], Hagit Zer [b], Marcela Parnes [a], Oshrat Harush-Frenkel [a], Jean Kadouche [c], Simon Benita [a,*,1]

[a] Department of Pharmaceutics, The Hebrew University of Jerusalem, Jerusalem, Israel
[b] Biacore Laboratory, The Hebrew University of Jerusalem, Jerusalem, Israel
[c] MAT Ltd., MAT Biopharma, Evry, France

ARTICLE INFO

Article history:
Received 15 June 2009
Accepted in revised form 30 September 2009
Available online 14 October 2009

Keywords:
Affinity constant
Cancer
Ferritin
Immunonanoparticles
Monoclonal antibody
Paclitaxel palmitate
Surface plasmon resonance

ABSTRACT

We have designed a site-specific drug colloidal carrier ultimately for improving pancreatic and lung cancer treatment. It is based on a nanoparticulate drug delivery system that targets tumors overexpressing H-ferritin. A monoclonal antibody, AMB8LK, specifically recognizing H-ferritin was thiolated and conjugated to maleimide-activated polylactide nanoparticles (NPs) resulting in the formation of immunonanoparticles (immunoNPs). The AMB8LK immunoNPs exhibited a mean diameter size of 112 ± 20 nm and a density of 76 antibody molecules per NP. AMB8LK immunoNPs were evaluated for uptake and binding properties on CAPAN-1 and A-549 cell lines, using confocal microscopy. ImmunoNPs demonstrated specific binding and increased uptake of the desired cells by means of monoclonal antibodies (MAbs), compared to nonconjugated NPs. A lipophilic paclitaxel derivative, paclitaxel palmitate (pcpl), was encapsulated within the various NP formulations, and their cytotoxic effect was evaluated on A-549 cells using MTT assay. Pcpl-loaded AMB8LK immunoNPs showed a significantly increased cytotoxic effect when compared to pcpl solution and pcpl NPs. Surface plasmon resonance (SPR) was used to determine quantitatively the affinity constants of native AMB8LK and AMB8LK immunoNPs to gain insight on the affinity of the MAbs following the conjugation process onto NPs. The results of the association/dissociation and affinity kinetics of the interaction between H-ferritin and native AMB8LK or AMB8LK immunoNPs revealed similar constant values, showing that the conjugation process of the MAb to the NPs did not alter the intrinsic specificity and affinity of the MAb to the antigen. In conclusion, at the cellular level, AMB8LK immunoNPs may carry drugs to desired overexpressing antigen cells with adequate affinity properties, potentially leading to improved drug therapy and reduced systemic adverse effects.

1. Introduction

Active targeting of nanoparticulate drug delivery systems has raised interest for improved cancer therapy. Monoclonal antibodies (MAbs) have been the most widely investigated targeting moieties following their conjugation to nanoparticles (NPs), which results in the formation of immunonanoparticles (immunoNPs) [1,2]. ImmunoNPs comprised of pegylated polyesters are considered to be the most suitable nanocarriers of chemotherapeutic agents to the tissue of interest, primarily due to their long circulating time [3,4], biodegradability, biocompatibility [5,6] and high drug payloads [7,8]. In addition to all these significant features, immunoNPs possess adequate physicochemical shelf life over long-term storage as freeze-dried powders, which can maintain their initial properties upon reconstitution with the addition of sterile water prior to use [9,10]. In previous reports, the physicochemical properties of drug-loaded immunoNPs have been evaluated in terms of type of covalent binding between the MAb to the NP, amount of MAbs attached to the NPs, recognition properties of immunoNPs on cultured cell lines and their ability to enhance cell internalization [11,12]. Recently, we designed polylactide (PLA) NPs loaded with the anti-cancer agent paclitaxel palmitate that were conjugated to an anti-HER-2 receptor MAb, trastuzumab [13]. These immunoNPs exhibited relatively high payloads of drug, excellent binding properties and significant cell uptake to HER-2 overexpressing cells. It was further observed in healthy mice that the pharmacokinetic behavior of the immunoNPs was markedly different from the pharmacokinetic profile of the naked MAb, demonstrating that the MAb lost its intrinsic

* Corresponding author. Tel.: +972 2 6758668; fax: +972 2 6757140.
E-mail address: benita@cc.huji.ac.il (S. Benita).
[1] Affiliated with the David R. Bloom Center for Pharmacy at The Hebrew University of Jerusalem, Israel.

0939-6411/$ - see front matter © 2009 Elsevier B.V. All rights reserved.
doi:10.1016/j.ejpb.2009.09.014

molecular pharmacokinetic properties following conjugation to the NPs. The immunoNPs elicited a significant anti-tumor activity in an orthotopic human prostate tumor induced in mice, when compared to the pcpl solution and NPs, although the tumor growth was not fully inhibited [13]. Despite these encouraging results, there was no accurate information on the damage elicited to the MAb following its conjugation to the NPs. It was then decided to carry out a quantitative investigation of the association and dissociation kinetics of immunoNPs to their antigen, when compared to the native MAb. For such a purpose, we applied the surface plasmon resonance (SPR) technique that has been used mainly in protein–ligand and antibody–antigen interaction studies. Although molecular interactions of antibody–antigen per se are well-established following numerous comprehensive affinities and kinetic analyses using SPR technique [14–16], they are not in the scope of the present manuscript. SPR allows real time analysis of molecular association between a MAb and an antigen and subsequent kinetic characteristics derived from the changes in refractive index close to a metal surface on which the antigen or the MAb is attached. When a molecule from the solution binds to the immobilized molecule on the metal surface, the resonance angle changes, and the response is recorded in a resonance unit (RU) [17,18]. Moreover, SPR has been used to investigate metal NPs for chemical sensing, imaging and targeting [19–21]. As an example, folic acid as a targeting moiety was conjugated to metal NPs and, its specific recognition by folic acid binding protein was demonstrated using SPR [22]. However, metal NPs cannot easily be used as drug delivery systems. It should be emphasized that SPR has been used to evaluate both qualitatively and quantitatively the affinity of antibodies attached to liposomes towards various antigens or receptors overexpressed in pathological tissues [23,24]. Furthermore, Kocbek and Coll. carried out a SPR study with anti-cytokeratin MAb attached covalently to NPs and evaluated the interaction of the immunoNPs with protein A [25]. The selected MAb in the present investigation is AMB8LK, which exhibits marked affinity for specific tumor organs overexpressing H-Ferritin [26]. It was previously demonstrated that total ferritin increased and shifted toward acidic (H-rich) ferritin [27] in the serum of patients with various malignancies such as colon cancer [28], testicular seminoma [29], breast cancer [30] and pancreatic cancer [31]. AMB8LK has been shown to exhibit marked affinity for specific tumor organs such as pancreatic and lung (NSCLC) cancers [32]. Moreover, a polyclonal antibody recognizing H-ferritin following coupling with yttrium 90 (Ferritarg P®) is currently under clinical evaluation in patients suffering relapsed or refractory Hodgkin's disease [33]. In this study, we have prepared and characterized immunoNPs conjugated to the anti-human H-ferritin AMB8LK MAb with or without the anti-cancer agent, paclitaxel palmitate. These immunoNPs were then evaluated on H-ferritin overexpressing cells for uptake, binding properties and cytotoxic effects. In the second part of this study, we have used SPR detection to monitor the reaction between these immunoNPs and their antigen, human H-ferritin. Here, we present a quantitative determination of immunoNPs' association and dissociation kinetics to their antigen when compared to the naked MAb.

2. Experimental

2.1. Materials

The polymer poly(ethylene glycol-co-lactide) MW 100,000 (PEG–PLA) was synthesized using the ring-opening polymerization method in the presence of stannous 2-ethylhexanoate as catalyst [34] and was described earlier [13].

Paclitaxel was purchased from Asia Talent Chemical, Shenzhen, China. Coumarin-6, Dimethyl sulfoxide (DMSO), 1-(4,5-Dimethylthiazol-2-yl)-3,5-diphenylformazan (MTT), 9-diethylamino-5H-benzo[α]phenoxazine-5-one (Nile Red) and polysorbate 80 (Tween® 80) were acquired from Sigma (St. Louis, MO, USA). Macrogol 15 hydroxystearate (Solutol® HS 15) was purchased from BASF (Ludwigshafen, Germany). FITC-labeled goat anti-mouse IgG and goat anti-mouse PE-labeled secondary antibodies were obtained from Jackson ImmunoResearch Laboratories (West Grove, PA, USA). Human Transferrin, Texas Red conjugated/tagged was obtained from Molecular Probes (Eugene, OR, USA). All organic solvents were HPLC grade and purchased from J.T. Baker (Deventer, Holland).

A research-grade CM5 (carboxymethyl dextran) sensor chip, NHS (*N*-hydroxysuccinimide), EDC [*N*-ethyl-*N*_-(3-dimethylaminopropyl)-carbodi-imide hydrochloride], ethanolamine/HCl and HBS-EP running buffer (10 mM Hepes, 150 mM NaCl, 3.4 mM EDTA and 0.005%, v/v, surfactant P20 at pH 7.4) were purchased from Biacore AB (Uppsala, Sweden). Human H-ferritin was obtained from Scripts (San Diego, CA, USA), while its MAb AMB8LK was a kind gift from MAT Biopharma (Evry, France). Human transferrin was purchased from Gibco (Invitrogen, Rockville, MD, USA).

2.2. Cell cultures

CAPAN-1 cell line (American Type Culture Collection, Rockville, MD, USA) was cultured in DMEM plus 20% fetal calf serum, 1% non-essential amino acids, 1% L-glutamine, 100 U/ml penicillin and 100 μg/ml streptomycin. Cells were maintained at 37 °C under 5% CO_2. A-549 cells (American Type Culture Collection, Rockville, MD) were grown in F-12K medium supplemented with 10% fetal calf serum, 1% L-glutamine, 100 U/ml penicillin and 100 μg/ml streptomycin. Cells were maintained at 37 °C under 5% CO_2. All cell culture products were obtained from Biological Industries (Kibbutz Beit Haemek, Israel).

2.3. Methods

2.3.1. Preparation of nonconjugated NPs or pcpl-loaded AMB8LK immunoNPs

The synthesis of pcpl [35] and the preparation of NPs and immunoNPs [13] were described in detail previously. In brief, mPEG–PLA MW 100,000 at a concentration of 0.6% w/v and the linker OMCCA at a concentration of 0.04% w/v were dissolved in 50 ml acetone containing 0.2% w/v Tween® 80. If pcpl-loaded immunoNPs were prepared, then 0.08% w/v of pcpl was added and dissolved into the organic phase. The organic phase was added to 100 ml of the aqueous phase which contained 0.1% w/v Solutol® HS 15. The suspension was stirred at 900 rpm over 1 h and then concentrated by evaporation to 10 ml. The formulations were adjusted to pH 8 and incubated overnight at 4 °C under nitrogen with thiolated AMB8LK MAb. The formulation was diafiltrated with 100 ml solution of 0.1% Tween® 80 (Vivaspin 300,000 MWCO, Vivascience, Stonehouse, UK) and filtered through 1.2 μm filters (FP 30/1.2 CA, Schleicher & Schuell, Dassel, Germany). When fluorescent NPs were needed, coumarin-6 was added to the organic phase resulting in a final concentration of 3 μg/ml.

2.3.2. AMB8LK immunoNP characterization

2.3.2.1. Particle size analysis. Mean diameter measurements of three batches of the same formulation was carried out utilizing an ALV Noninvasive Back Scattering High Performance Particle Sizer (ALV-NIBS HPPS, Langen, Germany) at 25 °C and using water as diluent. The sensitivity range was 0.5 nm to 5 μm.

2.3.2.2. Zeta potential measurements. The zeta potential of three batches of the same formulation was measured using the Malvern zetasizer (Malvern Instruments, Malvern, UK). The zeta potential measurement experiments were carried out in preliminary studies under different experimental conditions including water and low concentrations of NaCl solutions. Similar zeta potential values were obtained irrespective of the conditions. In view of the physical sensitivity of colloidal carriers to the presence of electrolytes, the remaining experiments were carried out using purified water (pH = 6 ± 0.16).

2.3.2.3. Transmission Electron Microscopy (TEM). Morphological evaluation of immunoNPs was performed by means of TEM (Philips Technai F20 100 KV). Specimens for TEM visualization were prepared by mixing the sample with phosphotungstic acid 2% (w/v) pH 6.4 for negative staining.

2.3.2.4. Drug incorporation. Pcpl-loaded AMB8LK immunoNPs were dissolved in acetonitrile, and the drug concentration was determined using the HPLC technique described previously [13]. Briefly, 20 μl of the acetonitrile samples were injected into an HPLC system (Kontron Instruments, Milan, Italy) consisting of a pump (422 Master), autosampler (model 360) and UV detector (model 332) with Lichrocart 100 RP-18 column (Merck, Darmstadt, Germany). Acetonitrile was used as the mobile phase, the identification of pcpl was obtained at the wavelength of 227 nm, and the retention time recorded was about 10 min.

2.3.3. Flow cytometry studies for H-ferritin identification on CAPAN-1 and A-549 cells

CAPAN-1 cells (human pancreatic adenocarcinoma) and A-549 cells (human lung carcinoma) were examined for human H-ferritin presence. Cells were cultured for several days and then harvested in 0.05% EDTA solution. Aliquots of cells (1×10^6) were fixed with 4% paraformaldehyde (PFA) solution in PBS over 30 min at 4 °C and washed three times with FACS buffer (1% w/v BSA and 0.02% w/v sodium azide in PBS pH 7.4) following incubation over 30 min at room temperature with 10% human sera in PBS. Cells were extensively washed with FACS buffer and incubated over 1 h at room temperature with increasing amounts of AMB8LK MAb (0.5–10 μg Ab per 10^6 cells), followed by incubation with goat anti-mouse PE-labeled secondary antibody over 1 h at room temperature. Following three additional wash steps with FACS buffer, these cells were resuspended into 1000 μl of FACS buffer. Cells were then analyzed for cell-associated fluorescence by determining the median fluorescence intensity (fluorescence per cell, in arbitrary units; MFI) of 10^4 cells aliquots using FACS (FACSCalibur, Becton Dickinson, NJ, USA).

2.3.4. In vitro binding and uptake studies to CAPAN-1 cells

Binding and uptake studies were carried out according to a conventional modified procedure [36]. Binding of AMB8LK immunoNPs to CAPAN-1 cells was confirmed by confocal laser scanning microscopy (CLSM). 300,000 CAPAN-1 cells were grown on coverslides in 12-well plates and incubated over 24 h at 37 °C and 5% CO_2 atmosphere to subconfluency. Cells were fixed with 4% PFA solution over 30 min at 4 °C and incubated with 1% BSA solution at ambient temperature. Following BSA solution removal, 30 μg of fluorescent NPs and fluorescent AMB8LK immunoNPs were incubated with cells over 1 h at 4 °C. Cells were washed three times with cold PBS, mounted on glass slides and observed with Olympus 1×70 confocal laser scanning microscope (Olympus Co. Ltd., Tokyo, Japan). The uptake of AMB8LK immunoNPs to CAPAN-1 cells was carried out in similar conditions excluding the fixation of cells, which was performed following the incubation of fluorescent formulations on live cells. Cells were mounted on glass slides and observed using confocal laser scanning microscopy (LSM410, Zeiss, Oberckochen, Germany). The fluorescence intensity of coumarin-6 incorporated in NPs was determined prior to cell incubation using Jasco-Spectrofluorometer (Model FP-770, Spectroscopic Co., Ltd., Hachioji City, Japan) following dissolution of the fluorescent NPs and immunoNPs in acetonitrile and was found to be equivalent at λ_{exc} 450 nm; λ_{em}s 495 nm.

2.3.5. In vitro uptake of AMB8LK immunoNPs to A-549 cells

The uptake of AMB8LK immunoNPs to A-549 cells was confirmed by confocal laser scanning microscopy (CLSM) according to a conventional modified procedure [36]. A-549 cells of 150,000 numbers were placed on coverslides in 12-well plates and incubated for 3 days at 37 °C and 5% CO_2 atmosphere to subconfluency. Cells were washed three times with MEM-0.6% BSA-Hepes, an acceptable cell media in endocytosis experiments in order to remove residual mucus and neutralize possible mucus effect. Coumarin-6-labeled NP formulations (30 μg) in MEM-BSA-Hepes were applied to the cells at 37 °C over 1 h. Cells were then washed three times using cold PBS and fixed using 4% PFA in PBS, washed extensively, mounted on glass slides and visualized by CLSM (Olympus Co. Ltd., Tokyo, Japan). Quantitative measurements of NP cell uptake, ruling out the possibility of calculating cell autofluorescence, was carried out according to the procedure described by Harush et al. [37,38]. All images were compiled using Adobe Photoshop, Adobe Illustrator and/or Image J software. The images are representative of the original data. Each experiment was performed in duplicate, and approximately six pictures were taken. Prior to cell incubation, the fluorescence intensity of coumarin-6 incorporated in NPs and immunoNPs was determined and found to be equivalent at λ_{exc} 450 nm; λ_{ems} 495 nm following their dissolution in acetonitrile using Jasco-Spectrofluorometer (Model FP-770, Spectroscopic Co., Ltd., Hachioji City, Japan). In support of cytoplasm visualization, following cell incubation with AMB8LK immunoNPs and with goat anti-mouse FITC-labeled secondary antibody, cells were incubated with media and with 1 μg of Nile Red solution in DMSO or with Texas Red conjugated to transferrin. Cells were visualized using CLSM (LSM410 Zeiss, Oberckochen, Germany).

2.3.6. In vitro cytotoxicity evaluation of AMB8LK immunoNPs on A-549 cells

A-549 cells of 100,000 numbers were seeded in 24-well tissue plates. Cells were grown for a period of two nights in full cell medium, including serum and antibiotics. Cells were washed with HBSS and incubated with various formulations diluted in full cell medium, for a period of 48 h at 37 °C. Following extensive washes with HBSS, cells were incubated with 0.5 mg/ml solution of MTT in HBSS over 1 h at 37 °C. MTT solution was discarded, and cells were incubated with DMSO for a period of 30 min at 37 °C. The absorbance of the samples was measured using a spectrophotometer ELISA plate reader (Powerwave ×340, Bio-tech Instruments Inc, VT, USA) at 570 nm.

2.3.6.1. Statistical analysis. Treatment effects were compared using one-way ANOVA followed by Tukey-Kramer Multiple Comparisons Test at pcpl concentrations ranging from 10 to 100 μM, using Instat GraphPad Software. Differences were considered significant if $P < 0.05$.

2.3.7. Preparation of sensor surfaces

All experiments were performed at 25 °C using SPR methodology. The kinetics and equilibrium constants for the interactions between human H-ferritin and AMB8LK immunoNPs were determined using the Biacore 3000 system (Biacore, Uppsala, Sweden). AMB8LK MAb and AMB8LK immunoNPs were immobilized on a CM5 sensor chip using amine-coupling chemistry [17]. The immobilization steps were carried out in PBS buffer at a flow rate of

10 μl/min. The surface was activated for 7 min with a mixture of 0.05 M NHS and 0.2 M EDC. AMB8LK and AMB8LK immunoNPs were injected at a concentration of 10 μg/ml in 10 mM acetate (pH 4) until the desired levels for the MAb and immunoNPs were achieved (600 and 500 RU, respectively). Ethanolamine (1 M, pH 8.5) was injected for 7 min to block the remaining activated groups. A control surface was prepared by activating the carboxyl groups and then blocking the activated groups by ethanolamine [17].

2.3.8. Biacore analysis

For the binding studies of the AMB8LK immunoNPs to H-ferritin, serial concentrations (0–200 nM) were injected through three flow cells (carrying AMB8LK, immunoNPs or a control) at a flow rate of 30 μl/min. The surface was regenerated after each interaction with a 10 μl pulse of 10 mM NaOH. The experiment was carried out in duplicate. The experiments were carried out using kinetics wizard of the Biacore Control Software (VERSION 3.1), which automatically corrects for refractive index changes and non-specific binding by subtracting the responses obtained for the control surface from the responses obtained in the tested samples. Kinetic and affinity analysis [39] was carried out when the resultant binding curves were fitted to the association and dissociation phases using Biacore evaluation software (version 4.1). In brief, the association constant is obtained from the reaction rate of the MAb–antigen complex formation, giving the number of complexes formed per time. As soon as the MAb–antigen complex is formed, its dissociation can commence. The dissociation rate constant expresses the number of complexes dissociating per unit time. The kinetic parameters are evaluated from association and dissociation phases of sensorgrams. The best fit was obtained from a simple bimolecular interaction of Langmuir 1:1 model, where the association rate constant and the dissociation rate constant were obtained from the following Eqs. (1) and (2), respectively. The affinity constant KD is the division result of K_d with K_a [39].

In another experiment, human transferrin was used as a negative control to verify the specificity binding of AMB8LK and AMB8LK immunoNPs to the H-ferritin.

$$\text{Association rate} = \frac{d[\text{AB}]}{dt} = K_a \times [\text{A}] \times [\text{B}] \quad (1)$$

$$\text{Dissociation rate} = \frac{-d[\text{AB}]}{dt} = K_d \times [\text{AB}] \quad (2)$$

where K_a is the association rate constant [$M^{-1}\ s^{-1}$], K_d the dissociation rate constant [s^{-1}], [A] the MAb concentration [M], [B] the antigen concentration [M], and [AB] is the MAb–antigen complex concentration [M].

3. Results

3.1. Characterization of AMB8LK immunoNPs

The well-established immunoNPs-manufacturing method yielded nanoparticles exhibiting a mean diameter size of 112 ± 20 nm and a negative zeta potential value of −21 ± 3 mV. The size distribution was further qualitatively confirmed by TEM observations (Fig. 1). The micrograph indicates that the immunoNPs obtained were individual polymeric particles, spherically shaped, homogeneous and nanometric. The MAb concentration conjugated to three batches of the same immunoNPs preparation was evaluated using the BCA protein assay kit (Pierce Chemical, Rockford IL, USA) and was found to be 0.78 ± 0.11 mg/ml. Based on the measured mean diameter of the immunoNPs and their concentration, the number of NPs was calculated. As stated earlier, the total number of MAb molecules conjugated to the NPs was determined experimentally. Thus, it was possible to calculate the average MAb density that was estimated to be 76 AMB8LK molecules per nanoparticle. When pcpl-loaded AMB8LK immunoNPs were prepared, the pcpl concentration in the colloidal dispersion measured by HPLC was found to be 2.8 mg/ml with drug content in the NPs of 9.6% w/w and a drug-loading efficiency of 70%.

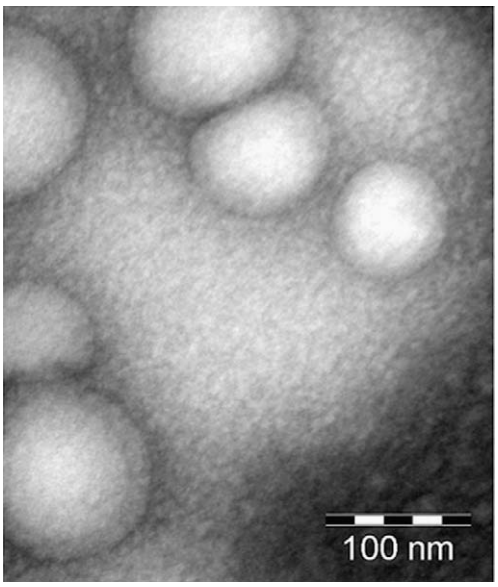

Fig. 1. Transmission electron microscopy microphotography of AMB8LK immunoNPs (at a density of 21 MAb molecules per particle). Specimen was prepared by mixing the sample with phosphotungstic 2%w/v pH 6.4 for negative staining.

3.2. Flow cytometry studies for H-ferritin identification on CAPAN-1 and A-549 cells

The results in Table 1 are presented in δ values, which are the ratio between the median fluorescence intensity of the cells incubated with MAb preparations and fluorescent probe, and the median fluorescence intensity of cells incubated with the fluorescent probe only. All the δ values are significantly larger than "1" following their incubation with increasing amounts of AMB8LK. The human H-ferritin (acidic) antigen overexpression in A-549 and CAPAN-1 cell lines was, therefore, validated by the results depicted in Table 1.

3.3. In vitro binding and uptake studies of AMB8LK immunoNPs to CAPAN-1 cells

The binding properties of AMB8LK immunoNPs were evaluated on the human H-ferritin overexpressing CAPAN-1 cell line. When the AMB8LK fluorescent coumarin-6 NPs were incubated with CAPAN-1 cells, the immunoNPs showed markedly increased binding properties (Fig. 2A) when compared to nonconjugated coumarin-6 NPs (data not shown). It was interesting to observe that even though the CAPAN-1 cell line overexpressed H-ferritin moderately when compared to A-549 cells, the targeted AMB8LK immunoNPs succeeded in binding to the cell membrane with significant affinity. In the case of cell uptake, the fluorescence intensity elicited by AMB8LK immunoNPs (Fig. 2C) within CAPAN-1 cells was much more pronounced, when compared to nonconjugated NPs (Fig. 2B). These findings establish the enhanced internalization of drug-loaded colloidal carrier to desired cells by means of MAbs.

3.4. In vitro uptake of AMB8LK immunoNPs to A-549 cells

CLSM observations showed that coumarin-6 AMB8LK immunoNPs (Fig. 3B) accumulated in the cells much more than coumarin-

Table 1
Human H-ferritin overexpression on CAPAN-1 and A-549 cell lines, presented as δ value, following incubation with increasing doses of AMB8LK MAb per 10^6 cells.

Cell line	δ value following incubation with AMB8LK MAb per 10^6 cells			
	0.5 μg	1 μg	2 μg	10 μg
A-549	22.1	34	30	20.5
CAPAN-1	2.42	2.74	2.92	3.9

6-labeled NPs (Fig. 3A). Internalization of AMB8LK immunoNPs when compared to the internalization of fluorescent NPs was approximately doubled, as noted from densitometry analyses of the cells (Fig. 3C). Cellular localization probes were incubated with A-549 cells following incubation with AMB8LK immunoNPs. It is clear from Fig. 3D that AMB8LK immunoNPs stained with FITC secondary MAb (green fluorescence) are localized in the cytosol stained with Nile red (red fluorescence) since marked orange staining of the cytosol is observed. The TxTr probe, which colors the endosomes in red, accumulates in the perinuclear compartment clearly differentiated from the green-labeled immunoNPs confirming the absence of the immunoNPs in the endosomes (Fig. 3E).

3.5. In vitro cytotoxicity evaluation of AMB8LK immunoNPs on A-549 cells

The feasibility of AMB8LK immunoNPs to target and deliver the anti-cancer agent pcpl to the human lung carcinoma cell line A-549 was evaluated in MTT studies. For this purpose, pcpl-loaded AMB8LK immunoNPs, pcpl NPs and pcpl solution at different concentrations (0.1–100 μM) were incubated for a period of 48 h with the cells. No cytotoxic effect of pcpl was detected up to 10 μM pcpl. When cells were incubated with increasing pcpl concentrations starting from 10 μM up to 100 μM, the immunoNPs exhibited a more effective cytotoxic effect on A-549 cells when compared to pcpl solution and pcpl NPs as depicted in Fig. 4 ($P < 0.001$ at 50, 100 μM and $P < 0.01$ at 10 μM). These results reveal the advantages of targeted delivery of anti-cancer drug to antigen overexpressing cells by means of MAbs.

3.6. Surface plasmon resonance

SPR technology was used to evaluate the association and dissociation properties of H-ferritin to AMB8LK conjugated to polymeric NPs when compared to native AMB8LK to confirm the MAb affinity postconjugation. The sensograms in Fig. 5 show the kinetic profiles of the interaction between H-ferritin and the native AMB8LK (Fig. 5A) or AMB8LK immunoNPs (Fig. 5B). Both sensograms exhibit similar association and dissociation profiles. The average kinetic parameters and the average affinity constants values are presented in Table 2. The association constant K_a and the dissociation constant K_d of AMB8LK and AMB8LK immunoNPs are close, resulting in similar affinity KD constants (6.67×10^{-9} and 8.16×10^{-9} M for the MAb and immunoNPs, respectively). This shows that the

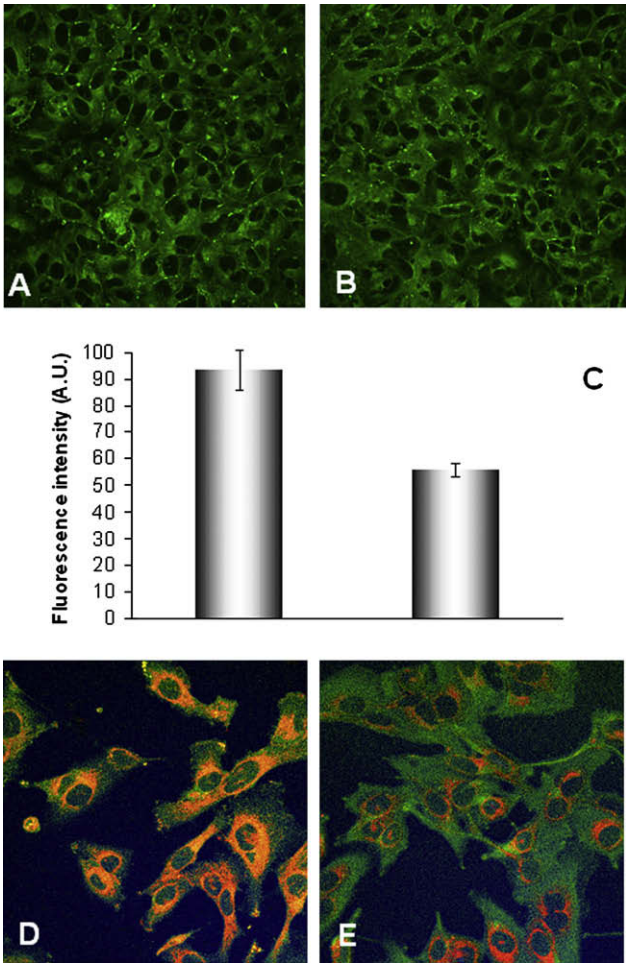

Fig. 3. Cellular uptake of coumarin-6-labeled NPs (A) and coumarin-6 AMB8LK immunoNPs (B) to A-549 cells as determined by CLSM. Cells were incubated with the formulation over 1 h at 37 °C. (C) Fluorescent intensities of internalized NPs and immunoNPs as analyzed by Image J software. Localization of AMB8LK immunoNPs in A-549 cells: following incubation with immunoNPs and anti-mouse FITC-labeled secondary antibody, cells were incubated with Nile Red (D) and with TxTr (E) cell fluorescent markers.

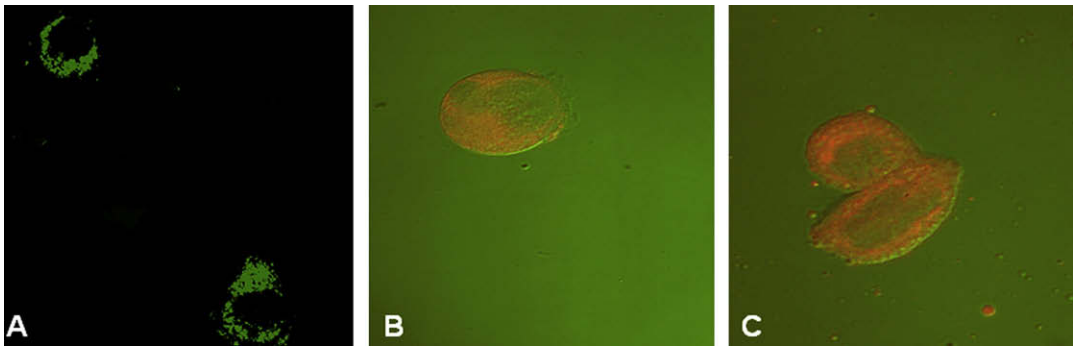

Fig. 2. Binding (A) and uptake (B and C) of coumarin-6-labeled immunoNPs to CAPAN-1 cells, as determined by CLSM. Binding following incubation at 4 °C over 1 h: (A) fluorescence microscopy of AMB8LK immunoNPs; uptake following incubation at 37 °C over 1 h: (B) fluorescent NPs; and (C) fluorescent AMB8LK immunoNPs.

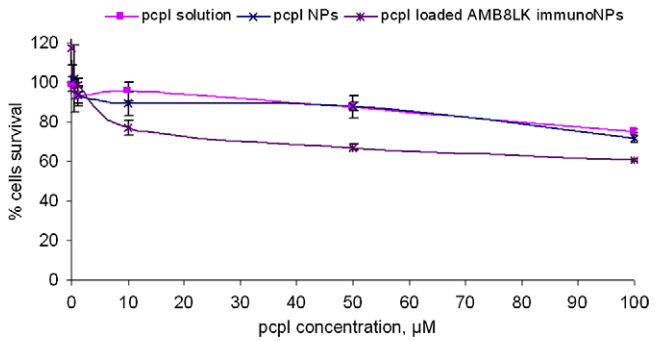

Fig. 4. Percentage of A-549 cell survival following incubation over a period of 48 h at 37 °C with AMB8LK immunoNPs, pcpl NPs and pcpl solution. Values are average ±SD. $N = 6$. $^{*}P$ value of Tukey-Kramer Multiple Comparisons was at least 0.001; $^{**}P$ value of Tukey-Kramer Multiple Comparisons was at least 0.01.

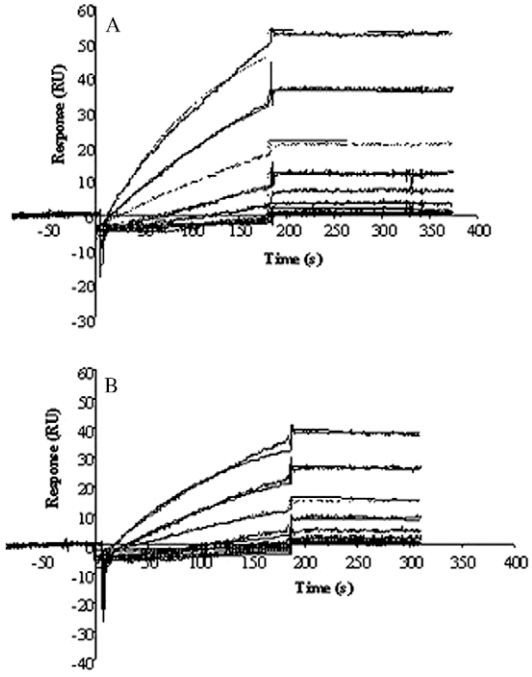

Fig. 5. Surface plasmon resonance sensograms showing the interaction curves of H-ferritin at different concentrations (0–200 nM) with (A) immobilized AMB8LK MAb and (B) immobilized AMB8LK immunoNPs.

Table 2
Average affinity constants obtained from the interaction between matrix-bound AMB8LK MAb or AMB8LK immunoNPs and H-ferritin solution.

Immobilized MAb	K_a (M^{-1} s^{-1})	K_d (s^{-1})	KD (M)
AMB8LK	3.45×10^4	1.53×10^{-4}	6.67×10^{-9}
AMB8LK immunoNPs	3.3×10^4	1.27×10^{-4}	8.16×10^{-9}

conjugation process of the MAb to the NP did not alter the MAb intrinsic binding properties, despite its covalent conjugation to the NPs. These results were further confirmed because no different kinetic behavior was noted when ferritin was immobilized and different concentrations of AMB8LK and AMB8LK immunoNPs were injected (data not shown).

To emphasize the specific binding of AMB8LK immunoNPs to H-ferritin and of AMB8LK to H-ferritin, we used transferrin, a different analyte. When AMB8LK and AMB8LK immunoNPs (Fig. 6A and B, respectively) were immobilized on the metal surface, an interaction with H-ferritin was detected at 1 μM while no interaction was observed with transferrin as analyte even at 8.5 μM. Thus, AMB8LK and AMB8LK immunoNPs recognize specifically ferritin only, validating the method used.

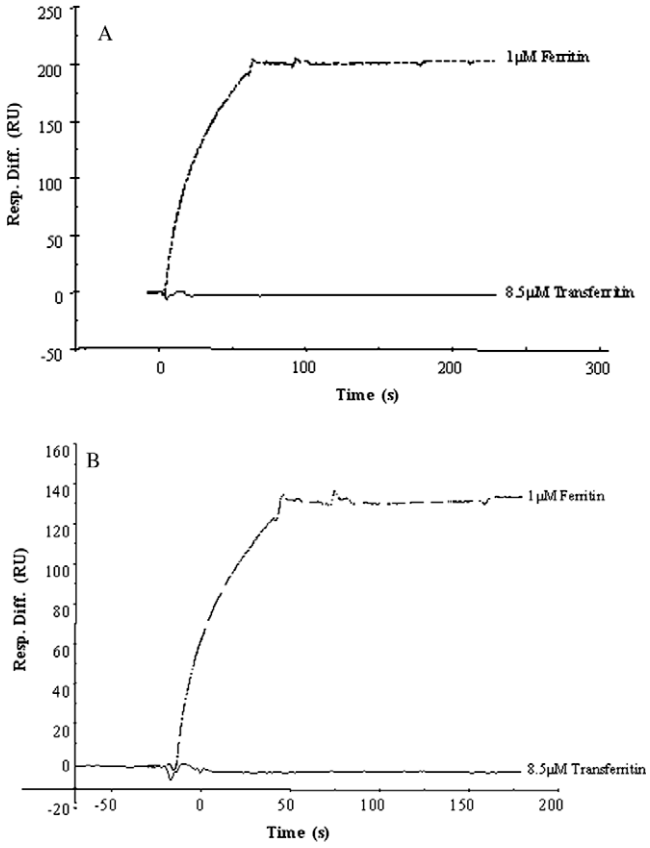

Fig. 6. Surface plasmon resonance sensograms showing the interaction curves of H-ferritin solution at concentration of 1 μM and of transferrin solution at concentration of 8.5 μM with (A) immobilized AMB8LK MAb and (B) immobilized AMB8LK immunoNPs.

4. Discussion

In an attempt to improve treatment in a few of the most challenging solid tumors, pancreatic and lung cancers [40,41], AMB8LK, a monoclonal antibody recognizing specifically H-ferritin, was conjugated to NPs. H-ferritin is a circulating protein; however, in various cancers, the level of H-ferritin increased markedly in tumor tissue versus comparable normal tissues [28–31]. Vriensendorp and Quadri [42] reported that in Hodgkin's disease, circulating ferritin levels are in the range of 500 ng/ml. Stochastic considerations indicate that iv administration of 2.5 mg rabbit anti-human ferritin IgG forms mainly one to one immune complexes in the circulation [43]. The antigen–antibody complex does not interfere with tumor targeting or lead to immune complex disease. Furthermore, Vriesendorp et al. [44] have shown in a clinical study that radiolabeled anti-ferritin targets tumor interstitium and shrinks tumor by radiation and not by immunologic effects in recurrent Hodgkin's disease patients. It should be stressed that the antibody used in the previous clinical studies was a polyclonal rabbit anti-human ferritin. Thus, theoretically, monoclonal anti-ferritin, as used in the present manuscript, should provide higher tumor uptake than polyclonal anti-ferritin. Furthermore, in a previous study where trastuzumab was conjugated to NPs using a conjugation process similar to the process used in the present study [13], the biofate following iv administration in healthy mice of trastuzumab immunoNPs when compared to nonconjugated NPs was investigated.

Both NP formulations were grafted with poly(ethylene glycol) (PEG) moieties on their surfaces. The results showed that the NP formulations were not captured by the reticuloendothelial system. Moreover, nonconjugated NPs and immunoNPs exhibited half-life values of 14.6 and 20 h, respectively, while the AUC values were 132.3 and 137.5 μg × h/ml, respectively. The in vivo pharmacokinetic profile and organ biodistribution even demonstrated that the conjugation of the MAb to the pegylated NPs conferred additional steric hindrance and prolonged the circulation time of the pegylated immunoNPs when compared to pegylated NPs [13]. It was interesting to note that when the two MAbs, AMB8LK and trastuzumab [13] were conjugated to NPs under identical experimental conditions including the initial concentrations of the antibodies, the characterization of the various immunoNPs revealed that the physicochemical properties were similar, with the exception of the density. Whereas in the previous study, only 43 trastuzumab molecules were conjugated per NP [13]; in this study, 76 MAbs of AMB8LK were conjugated per NP. The marked increase in AMB8LK density on the NP when compared to trastuzumab, despite the identical number of thiol groups on each MAb molecule, can be attributed to the different molecular structure of AMB8LK that led to a more favorable conformation, resulting in a better exposure of the sulfhydryl groups available for conjugation with the maleimide groups on the active nanoparticles surface. It can be deduced from the high δ values depicted in Table 1 that A-549 cells elicited a marked overexpression of H-ferritin over CAPAN-1 cells. When A-549 cells were incubated with 1 μg AMB8LK, the δ value showed a marked increase of 154% when compared to incubation with 0.5 μg MAb. However, when higher amounts of 2 and 10 μg MAb were incubated with A-549 cells, the δ value decreased, indicating a possible saturation process of MAb conjugated to H-ferritin. The decrease in δ values can be attributed to molecular hindrance occurring at high MAb concentrations, leading to lower binding to H-ferritin. When AMB8LK was incubated with CAPAN-1 cells, the δ values showed moderate overexpression of H-ferritin compared to A-549, and no saturation was observed since δ values increased progressively with increasing amounts of MAb up to 10 μg. Nevertheless, in view of the results depicted in Table 1, the presence of the human H-ferritin antigen has been verified in the A-549 non-small cell lung cancer in vitro model [45]. Therefore, an anti-H-ferritin MAb such as AMB8LK is a suitable means to target non-small cell lung cancer and spare normal cells. This concept was further established in the cell uptake study (Fig. 3), when fluorescent AMB8LK immunoNPs were found to accumulate in the cells approximately two times more than fluorescent NPs. The binding and uptake studies in CAPAN-1 cell line revealed specific affinity of AMB8LK immunoNPs towards the human pancreatic cancerous cells (Fig. 2). To demonstrate the presence of AMB8LK immunoNPs in the cell cytoplasm, cells were incubated with two cell markers: Nile Red which stains intracellular lipid droplets in red [46,47] and Texas Red conjugated to human transferrin (TxTr) which is a marker of endosomes following receptor-mediated endocytosis [48,49]. The green fluorescence emitted by the AMB8LK immunoNPs overlapped with the red fluorescence emitted by the cytosol as depicted in Fig. 3D, indicating that the immunoNPs are localized within the cell cytoplasm, in association with the cells' lipid droplets. It could also be deduced that AMB8LK immunoNPs did not enter or escape from the endosomes within the 1-h incubation period since the green fluorescence emitted by the immunoNPs did not co-localize with the red fluorescence emitted by the endosome probe, TxTr (Fig. 3E). The in vitro cytotoxic effect of pcpl-loaded AMB8LK immunoNPs at different drug concentrations on lung cancer cells is depicted in Fig. 4. The immunoNPs were more effective than pcpl NPs or pcpl solution, probably as a result of the extensive cell uptake of the immunoNPs as shown in Fig. 3C. It should be emphasized that the activity of paclitaxel palmitate was found to be equivalent to the activity of paclitaxel [35]. Normally, as also reported by other authors, the conventional approach to verify whether the conjugation process altered the initial affinity of the native MAb is to evaluate the binding and uptake in cell cultures [11,12]. Although cell culture findings are positive and encouraging, these results remain qualitative and do not provide clear information, at least quantitatively, to how the native binding affinity of the MAb has been affected by the coupling reaction and formation of the immunoNPs. Thus, SPR analysis was applied in the present case to quantitatively assess the effect of the conjugation process on the MAb activity. SPR is a well-known and established technique to evaluate the affinity between antigens and antibodies, providing mass balance accurate calculations for the production of the FDA-approved antibodies following biopharmaceutical manufacturing processes [50,51]. The SPR study of Fab′ fragment of anti-ferritin MAb with ferritin was reported [52]. The authors found that when ferritin was immobilized, the K_a and K_d values were $8.3 \times 10^4\ M^{-1}s^{-1}$ and $1.2 \times 10^{-3}\ s^{-1}$, respectively, resulting in a calculated KD value of 1.4×10^{-8} M. This value is moderately higher than the KD value of 6.67×10^{-9} M of the AMB8LK MAb presented in Table 2. The discrepancy in the values is probably due to the difference in the nature of the two antibodies that recognize different epitopes. First attempts to evaluate the affinity kinetics of the binding of IOT4a MAb adsorbed on NPs to its antigen, rsCD4, by SPR were reported by Velge-Roussel [53]. The authors reported that the adsorption process did not prevent the specific recognition of the MAb to rsCD4 with K_d value of $0.004\ s^{-1}$. However, the authors did not report any comparison with the native MAb, assuming that the rate of IOT4a–rsCD4 binding was the same for free MAb as for MAb adsorbed on NPs. Other authors investigated using SPR, the interaction of immobilized protein A to anti-cytokeratin MAb either adsorbed or covalently linked to PLGA NPs [54]. Comparable studies to our actual study investigating the quantitative comparison of free MAb–antigen interaction or MAbs covalently attached to NPs–antigen interaction using SPR were carried out with immunoliposomes. When the antigen Ox_{16}BSA was immobilized, immunoliposomes conjugated to Ox lpp-scFv-H6 displayed specific hapten-binding activity, but the affinity constants were not measured [23]. In another study, the KD value of F5 anti-ErbB2 immunoliposomes was found to be 111 nM, while the KD value of soluble, unconjugated F5 scFv to ErbB2 was 160 nM, showing qualitatively that the antibody conjugation to the liposome does not significantly affect the monovalent interaction with F5 scFv [24]. These findings are in agreement with the results presented in this study. The actual results clearly indicate that the thioether bond formed between the thiolated MAbs and maleimide surface-activated NPs is efficient and does not impair the affinity of the MAb towards its antigen. It can thus be deduced that appropriate experimental conditions have been identified to covalently attach AMB8LK to PEG–PLA NPs comprising a chemotherapeutic drug and resulting in a potential improved antibody drug-targeted delivery system that may be used in the treatment of pancreatic and lung cancers.

Acknowledgment

Part of this study was supported by a grant from the European Community (STREP 2005-518185).

References

[1] J.C. Olivier, R. Huertas, H.J. Lee, F. Calon, W.M. Pardridge, Synthesis of pegylated immunonanoparticles, Pharmaceutical Research 19 (8) (2002) 1137–1143.
[2] D. Bourel, A. Rolland, R. Le Verge, B. Genetet, A new immunoreagent for cell labeling. CD3 monoclonal antibody covalently coupled to fluorescent polymethacrylic nanoparticles, Journal of Immunological Methods 106 (2) (1988) 161–167.

[3] K. Avgoustakis, A. Beletsi, Z. Panagi, P. Klepetsanis, E. Livaniou, G. Evangelatos, D.S. Ithakissios, Effect of copolymer composition on the physicochemical characteristics, in vitro stability, and biodistribution of PLGA-mPEG nanoparticles, International Journal of Pharmaceutics 259 (1–2) (2003) 115–127.
[4] M. Tobio, A. Sanchez, A. Vila, I.I. Soriano, C. Evora, J.L. Vila-Jato, M.J. Alonso, The role of PEG on the stability in digestive fluids and in vivo fate of PEG–PLA nanoparticles following oral administration, Colloids and Surfaces 18 (3–4) (2000) 315–323.
[5] S. Stolnik, S.E. Dunn, M.C. Garnett, M.C. Davies, A.G. Coombes, D.C. Taylor, M.P. Irving, S.C. Purkiss, T.F. Tadros, S.S. Davis, et al., Surface modification of poly(lactide-co-glycolide) nanospheres by biodegradable poly(lactide)-poly(ethylene glycol) copolymers, Pharmaceutical Research 11 (12) (1994) 1800–1808.
[6] K.S. Soppimath, T.M. Aminabhavi, A.R. Kulkarni, W.E. Rudzinski, Biodegradable polymeric nanoparticles as drug delivery devices, Journal of Control Release 70 (1–2) (2001) 1–20.
[7] I. Brigger, C. Dubernet, P. Couvreur, Nanoparticles in cancer therapy and diagnosis, Advanced Drug Delivery Reviews 54 (5) (2002) 631–651.
[8] C. Fonseca, S. Simoes, R. Gaspar, Paclitaxel-loaded PLGA nanoparticles: preparation, physicochemical characterization and in vitro anti-tumoral activity, Journal of Control Release 83 (2) (2002) 273–286.
[9] Y.N. Konan, R. Gurny, E. Allemann, Preparation and characterization of sterile and freeze-dried sub-200 nm nanoparticles, International Journal of Pharmaceutics 233 (1–2) (2002) 239–252.
[10] F. De Jaeghere, E. Allemann, J.C. Leroux, W. Stevels, J. Feijen, E. Doelker, R. Gurny, Formulation and lyoprotection of poly(lactic acid-co-ethylene oxide) nanoparticles: influence on physical stability and in vitro cell uptake, Pharmaceutical Research 16 (6) (1999) 859–866.
[11] N. Dinauer, S. Balthasar, C. Weber, J. Kreuter, K. Langer, H. von Briesen, Selective targeting of antibody-conjugated nanoparticles to leukemic cells and primary T-lymphocytes, Biomaterials 26 (29) (2005) 5898–5906.
[12] Y. Akasaka, H. Ueda, K. Takayama, Y. Machida, T. Nagai, Preparation and evaluation of bovine serum albumin nanospheres coated with monoclonal antibodies, Drug Design Delivery 3 (1) (1988) 85–97.
[13] N. Debotton, M. Parnes, J. Kadouche, S. Benita, Overcoming the formulation obstacles towards targeted chemotherapy: in vitro and in vivo evaluation of cytotoxic drug loaded immunonanoparticles, Journal of Control Release 127 (3) (2008) 219–230.
[14] P. Torreri, M. Ceccarini, P. Macioce, T.C. Petrucci, Biomolecular interactions by surface plasmon resonance technology, Annali dell'Istituto superiore di sanita 41 (4) (2005) 437–441.
[15] W. Huber, F. Mueller, Biomolecular interaction analysis in drug discovery using surface plasmon resonance technology, Current Pharmaceutical Design 12 (31) (2006) 3999–4021.
[16] M.H. Van Regenmortel, L. Choulier, Recognition of peptides by antibodies and investigations of affinity using biosensor technology, Combinatorial Chemistry & High Throughput Screening 4 (5) (2001) 385–395.
[17] B. Johnsson, S. Lofas, G. Lindquist, Immobilization of proteins to a carboxymethyldextran-modified gold surface for biospecific interaction analysis in surface plasmon resonance sensors, Analytical Biochemistry 198 (2) (1991) 268–277.
[18] B. Johnsson, S. Lofas, G. Lindquist, A. Edstrom, R.M. Muller Hillgren, A. Hansson, Comparison of methods for immobilization to carboxymethyl dextran sensor surfaces by analysis of the specific activity of monoclonal antibodies, Journal of Molecular Recognition 8 (1–2) (1995) 125–131.
[19] C.J. Murphy, A.M. Gole, S.E. Hunyadi, J.W. Stone, P.N. Sisco, A. Alkilany, B.E. Kinard, P. Hankins, Chemical sensing and imaging with metallic nanorods, Chemical Communications (5) (2008) 544–557.
[20] X. Huang, P.K. Jain, I.H. El-Sayed, M.A. El-Sayed, Gold nanoparticles: interesting optical properties and recent applications in cancer diagnostics and therapy, Nanomedicine 2 (5) (2007) 681–693.
[21] J. Wang, H.S. Zhou, Aptamer-based au nanoparticles-enhanced surface plasmon resonance detection of small molecules, Analytical Chemistry 80 (18) (2008) 7174–7178.
[22] F. Sonvico, S. Mornet, S. Vasseur, C. Dubernet, D. Jaillard, J. Degrouard, J. Hoebeke, E. Duguet, P. Colombo, P. Couvreur, Folate-conjugated iron oxide nanoparticles for solid tumor targeting as potential specific magnetic hyperthermia mediators: synthesis, physicochemical characterization, and in vitro experiments, Bioconjugate Chemistry 16 (5) (2005) 1181–1188.
[23] M.L. Laukkanen, K. Alfthan, K. Keinanen, Functional immunoliposomes harboring a biosynthetically lipid-tagged single-chain antibody, Biochemistry 33 (38) (1994) 11664–11670.
[24] U.B. Nielsen, D.B. Kirpotin, E.M. Pickering, K. Hong, J.W. Park, M. Refaat Shalaby, Y. Shao, C.C. Benz, J.D. Marks, Therapeutic efficacy of anti-ErbB2 immunoliposomes targeted by a phage antibody selected for cellular endocytosis, Biochimica et Biophysica Acta 1591 (1–3) (2002) 109–118.
[25] P. Kocbek, N. Obermajer, M. Cegnar, J. Kos, J. Kristl, Targeting cancer cells using PLGA nanoparticles surface modified with monoclonal antibody, Journal of Control Release 120 (1–2) (2007) 18–26.
[26] R.L.J. Kadouche, Use of anti-ferritin monoclonal antibodies in the treatment of some cancers USA Patent 2006.
[27] J.T. Hazard, J.W. Drysdale, Ferritinaemia in cancer, Nature 265 (5596) (1977) 755–756.
[28] A. Harrison, C.A. Walker, D. Parker, K.J. Jankowski, J.P. Cox, A.S. Craig, J.M. Sansom, N.R. Beeley, R.A. Boyce, L. Chaplin, et al., The in vivo release of 90Y from cyclic and acyclic ligand–antibody conjugates, International Journal of Radiation Applications and Instrumentation 18 (5) (1991) 469–476.
[29] L. Camera, S. Kinuya, K. Garmestani, C. Wu, M.W. Brechbiel, L.H. Pai, T.J. McMurry, O.A. Gansow, I. Pastan, C.H. Paik, et al., Evaluation of the serum stability and in vivo biodistribution of CHX-DTPA and other ligands for yttrium labeling of monoclonal antibodies, Journal of Nuclear Medicine 35 (5) (1994) 882–889.
[30] G. Guner, G. Kirkali, C. Yenisey, I.R. Tore, Cytosol and serum ferritin in breast carcinoma, Cancer Letters 67 (2–3) (1992) 103–112.
[31] J.W. Drysdale, T.G. Adelman, P. Arosio, D. Casareale, P. Fitzpatrick, J.T. Harzard, M. Yokota, Human isoferritins in normal and disease states, Seminars in Hematology 14 (1) (1977) 71–88.
[32] E.N. Sabbah, J. Kadouche, D. Ellison, C. Finucane, D. Decaudin, S.J. Mather, In vitro and in vivo comparison of DTPA- and DOTA-conjugated antiferritin monoclonal antibody for imaging and therapy of pancreatic cancer, Nuclear Medicine and Biology 34 (3) (2007) 293–304.
[33] D. Decaudin, R. Levy, F. Lokiec, F. Morschhauser, M. Djeridane, J. Kadouche, A. Pecking, Radioimmunotherapy of refractory or relapsed Hodgkin's lymphoma with 90Y-labelled antiferritin antibody, Anti-cancer Drugs 18 (6) (2007) 725–731.
[34] D. Bazile, C. Prud'homme, M.T. Bassoullet, M. Marlard, G. Spenlehauer, M. Veillard, Stealth Me.PEG–PLA nanoparticles avoid uptake by the mononuclear phagocytes system, Journal of Pharmaceutical Sciences 84 (4) (1995) 493–498.
[35] D. Goldstein, O. Gofrit, A. Nyska, S. Benita, Anti-HER2 cationic immunoemulsion as a potential targeted drug delivery system for the treatment of prostate cancer, Cancer Research 67 (1) (2007) 269–275.
[36] E. Harlow, D. Lane, Antibodies Laboratory Manual, Cold Spring Harbor Laboratory Press, New York, 1988.
[37] O. Harush-Frenkel, N. Debotton, S. Benita, Y. Altschuler, Targeting of nanoparticles to the clathrin-mediated endocytic pathway, Biochemical and Biophysical Research Communications 353 (1) (2007) 26–32.
[38] O. Harush-Frenkel, E. Rozentur, S. Benita, Y. Altschuler, Surface charge of nanoparticles determines their endocytic and transcytotic pathway in polarized MDCK cells, Biomacromolecules 9 (2) (2008) 435–443.
[39] BIACORE, Introduction to Kinetic & Affinity Analysis. GE Healthcare, 2008. <http://www.biacore.com/lifesciences/index.html>.
[40] R. Talar-Wojnarowska, E. Malecka-Panas, Molecular pathogenesis of pancreatic adenocarcinoma: potential clinical implications, Medical Science Monitor 12 (9) (2006) RA186–RA193.
[41] D.K. Espey, X.C. Wu, J. Swan, C. Wiggins, M.A. Jim, E. Ward, P.A. Wingo, H.L. Howe, L.A. Ries, B.A. Miller, A. Jemal, F. Ahmed, N. Cobb, J.S. Kaur, B.K. Edwards, Annual report to the nation on the status of cancer, 1975–2004, featuring cancer in American Indians and Alaska Natives, Cancer 110 (10) (2007) 2119–2152.
[42] H.M. Vriesendorp, S.M. Quadri, Radiolabeled immunoglobulin therapy: old barriers and new opportunities, Expert Review of Anticancer Therapy 1 (3) (2001) 461–478.
[43] J. Lai, S.M. Quadri, P.E. Borchardt, L. Harris, R. Wucher, E. Askew, L. Schweichel, H.M. Vriesendorp, Pharmacokinetics of radiolabeled polyclonal antiferritin in patients with Hodgkin's disease, Clinical Cancer Research 5 (Suppl. 10) (1999) 3315s–3323s.
[44] H.M. Vriesendorp, S.M. Quadri, B.S. Andersson, C.T. Wyllie, K.A. Dicke, Recurrence of Hodgkin's disease after indium-111 and yttrium-90 labeled antiferritin administration, Cancer 80 (Suppl.12) (1997) 2721–2727.
[45] R.J. Phillips, J. Mestas, M. Gharaee-Kermani, M.D. Burdick, A. Sica, J.A. Belperio, M.P. Keane, R.M. Strieter, Epidermal growth factor and hypoxia-induced expression of CXC chemokine receptor 4 on non-small cell lung cancer cells is regulated by the phosphatidylinositol 3-kinase/PTEN/AKT/mammalian target of rapamycin signaling pathway and activation of hypoxia inducible factor-1alpha, The Journal of Biological Chemistry 280 (23) (2005) 22473–22481.
[46] M.K. McMillian, E.R. Grant, Z. Zhong, J.B. Parker, L. Li, R.A. Zivin, M.E. Burczynski, M.D. Johnson, Nile Red binding to HepG2 cells: an improved assay for in vitro studies of hepatosteatosis, In vitro & Molecular Toxicology 14 (3) (2001) 177–190.
[47] D. Wustner, N.J. Faergeman, Chromatic aberration correction and deconvolution for UV sensitive imaging of fluorescent sterols in cytoplasmic lipid droplets, Cytometry A (2008).
[48] V. Blot, T.E. McGraw, GLUT4 is internalized by a cholesterol-dependent nystatin-sensitive mechanism inhibited by insulin, The EMBO Journal 25 (24) (2006) 5648–5658.
[49] M. Guyader, E. Kiyokawa, L. Abrami, P. Turelli, D. Trono, Role for human immunodeficiency virus type 1 membrane cholesterol in viral internalization, Journal of Virology 76 (20) (2002) 10356–10364.
[50] P. Thillaivinayagalingam, A.R. Newcombe, K. O'Donovan, R. Francis, E. Keshavarz-Moore, Detection and quantification of affinity ligand leaching and specific antibody fragment concentration within chromatographic fractions using surface plasmon resonance, Biotechnology and Applied Biochemistry 48 (Pt 4) (2007) 179–188.
[51] A. Ahmad, A. Ramakrishnan, M.A. McLean, A.P. Breau, Use of surface plasmon resonance biosensor technology as a possible alternative to detect differences in binding of enantiomeric drug compounds to

immobilized albumins, Biosensors & Bioelectronics 18 (4) (2003) 399–404.
[52] G.W. Oddie, L.C. Gruen, G.A. Odgers, L.G. King, A.A. Kortt, Identification and minimization of nonideal binding effects in BIAcore analysis: ferritin/anti-ferritin Fab′ interaction as a model system, Analytical Biochemistry 244 (2) (1997) 301–311.
[53] F. Velge-Roussel, P. Breton, X. Guillon, F. Lescure, N. Bru, D. Bout, J. Hoebeke, Immunochemical characterization of antibody-coated nanoparticles, Experientia 52 (8) (1996) 803–806.
[54] N. Obermajer, P. Kocbek, U. Repnik, A. Kuznik, M. Cegnar, J. Kristl, J. Kos, Immunonanoparticles – an effective tool to impair harmful proteolysis in invasive breast tumor cells, The FEBS Journal 274 (17) (2007) 4416–4427.